Spatial Correlation Singularity of a Vortex Field

D. M. Palacios, I. D. Maleev, A. S. Marathay, and G. A. Swartzlander, Jr.

Optical Sciences Center, University of Arizona, Tucson, Arizona 85721, USA
(Received 21 October 2003; published 9 April 2004)

Experimental and numerical techniques allowed us to predict and verify the existence of a robust phase singularity in the spatial coherence function when a vortex is present. Though observed in the optical domain, this phenomenon may occur in any partially coherent vortex wave.

The space-time evolution of a wave is governed by its phase front topology. A wave having a helical phase front may be called a "vortex wave" owing to the circulation of momentum around the helix axis [1]. The last decade has seen a resurgence of interest in optical vortices [2], owing in part to readily available computer-generated holographic [3–5] or lithographic [6,7] techniques for creating vortices in laser beams. Vortex waves are known to occur in coherent systems having a well-defined phase, but are ill defined in partially coherent systems where statistics are required to quantify the phase. In the incoherent limit neither the helical phase nor the characteristic "eye" in the intensity profile is observable. Here we explore the vortex state and its statistical properties when the beam has arbitrary spatial coherence.

Optics affords a convenient means to vary the spatial coherence properties by changing the apparent size of an incoherent source as viewed in the detection plane. Recently, several groups have explored the theoretical and practical properties of optical vortices formed in partially coherent light. Certain classes of partially coherent beams carefully constructed to carry optical vortex modes have been examined analytically [8–10] and experimentally [11]. Zeros with [12] and without [13] a vortex phase structure were predicted to occur in the two-point correlation function. Coherence filtering techniques were proposed [14] and verified [15] as a means to measure a weak incoherent signal lost in the glare of a stronger coherent source.

In this Letter, we use experimental and numerical techniques to explore how a beam transmitted through a vortex phase mask changes as the transverse coherence length at the input of the mask is changed. We assume a quasimonochromatic, statistically stationary light source and ignore temporal coherence effects. We demonstrate that, although the characteristic dark core of a vortex fills with diffuse light with decreasing coherence, robust attributes of the vortex remain in the beam, most prominently in the form of a ring dislocation in the cross-correlation function.

For a coherent wave, a single optical vortex in a scalar beam may be expressed in cylindrical coordinates (r, ϕ, z) [16]:

$$E(r, \phi, z, t) = A(r, z) \exp(im\phi) \exp(i\omega t - ikz), \quad (1)$$

where $A(r, z)$ is the field amplitude, m is the topological charge of the vortex, ω is the angular frequency, and k is the wave number. The vortex nature of the field is governed by the phase factor $\exp(im\phi)$. At a fixed instant of time, helical surfaces of constant phase given by $m\phi - kz = \text{const}$ are produced. The amplitude vanishes along the helix axis ($r = 0$) owing to destructive interference in the vicinity of the vortex core, i.e., $A(0, z) = 0$. For computational simplicity in the discussion below we consider a vortex with the initial field amplitude of a Laguerre-Gaussian mode:

$$A(r, z = 0) = E_0(r/w)^m \exp(-r^2/w^2) \exp(i\beta), \quad (2)$$

where E_0 and w are the characteristic amplitude and beam size in the plane $z = 0$, and β is an arbitrary phase.

A planar ($m = 0$) beam can be converted into a vortex beam by transmitting the light through a transparent diffractive phase mask having a thickness given by $d = d_0 - m\lambda_0\phi/2\pi(n_s - n_0)$, where d_0 is the nominal thickness, λ_0 is the wavelength for which the mask is intended, n_s is the refractive index of the substrate, and n_0 is the index of refraction of the surrounding medium.

A partially coherent beam propagating through a vortex mask may be expected to gain the characteristic vortex phase factor $\exp(im\phi)$ even though the wave front is not well defined. For example, if we view an incoherent beam as an incoherent superposition of coherent beams each having a random phase $\tilde{\beta}$, then each coherent beam will gain a vortex phase factor. A schematic diagram of a partially coherent beam of light transmitted through a vortex mask is shown in Fig. 1. Here we assume an incoherent source of diameter D_s a distance z_s from a vortex mask of radial size w in the plane $z = 0$. A measure of the spatial coherence of a single beam of light in the plane $z = 0$ may be found by calculating the mutual coherence function (MCF)[17] of the electric field for points in the transverse plane, $\vec{r}_1$ and $\vec{r}_2$ (see Fig. 1),

$$\Gamma(\vec{r}_1, \vec{r}_2) = \langle E(\vec{r}_1, t)E^*(\vec{r}_2, t)\rangle, \quad (3)$$

where $\langle\rangle$ denotes an ensemble average. For computational convenience we assume that the statistical distribution of the phase $\tilde{\beta}$ in the plane $z = 0$ corresponds to a Carter-Wolf type light source having a Gaussian-Schell correlator
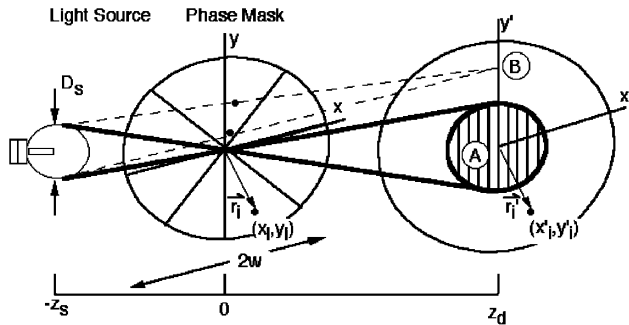
FIG. 1. A diagram of a partially coherent beam of light transmitted through a vortex mask of transverse diameter $2w$. In the plane $z = z_d$, a conical projection of the source through the center of the mask forms an enclosed circular region. Light inside the circle (point A) contains rays from all sectors of the mask, but outside the circle (point B) the light contains rays from only adjacent sectors of the mask, as depicted by the dashed lines.

$$C(|\vec{r}_1 - \vec{r}_2|) = \exp[-|\vec{r}_1 - \vec{r}_2|^2/L_c^2], \qquad (4)$$

where L_c is the transverse coherence length at $z = 0$. Using Eqs. (1) and (2) the MCF may be written

$$\Gamma(\vec{r}_1, \vec{r}_2) = C(|\vec{r}_1 - \vec{r}_2|)E_0^2|\vec{r}_1 \cdot \vec{r}_2/w^2|^m \exp[-(r_1^2 + r_2^2)/w^2]$$
$$\times \exp[-im(\phi_1 - \phi_2)]. \qquad (5)$$

The MCF in the detection plane (see Fig. 1) after the beam has propagated a distance z_d is given by [17]

$$\Gamma'(\vec{r}_1', \vec{r}_2') = a \iiiint \Gamma(\vec{r}_1, \vec{r}_2)\rho_1^{-3}\rho_2^{-3}(1 - ik\rho_1)(1 + ik\rho_2)$$
$$\times \exp[ik(\rho_1 - \rho_2)]d\vec{r}_1 d\vec{r}_2, \qquad (6)$$

where $\rho_i = [|\vec{r}_i' - \vec{r}_i|^2 + z_d^2]^{1/2}$ $(i = 1, 2)$ and $a = z_d^2/4\pi^2$. As we will show, the most striking statistical feature of a propagated vortex formed in a partially coherent beam is that the cross-correlation function, $\chi'(\vec{r}') \equiv \Gamma'(\vec{r}_1', -\vec{r}_1')$, is a more robust pattern than the intensity (the autocorrelation function), $I'(\vec{r}') \equiv \Gamma'(\vec{r}_1', \vec{r}_1')$.

A geometric description of rays passing through various sectors of the mask will serve to develop an understanding of the nature of the beam as it propagates. Consider first the correlation function in the plane of the mask, $\Gamma(\vec{r}_1, \vec{r}_2)$. According to Eq. (5), the points $\vec{r}_1$ and $\vec{r}_2$ are positively correlated (i.e. $\mathrm{Re}[\Gamma(\vec{r}_1, \vec{r}_2)] > 0$) if the phase difference between them obeys the relation, $m|\phi_2 - \phi_1| \leq \pi/2$, otherwise the points are anticorrelated (i.e. $\mathrm{Re}[\Gamma(\vec{r}_1, \vec{r}_2)] < 0$). Note that if the mask is removed (i.e., if $m = 0$), $\Gamma(\vec{r}_1, \vec{r}_2)$ is everywhere real and positive. Let us now examine light in the plane $z = z_d$. This correlation/anticorrelation distinction is carried with the beam as it propagates and may be geometrically described as a conical projection of the light source through the center of the mask. This cone defines a circle,

shown in the (x', y') plane in Fig. 1, forming a correlation/anticorrelation boundary. The size of this boundary may be expected to increase with increasing beam spread, and thus it depends on both the size of the source (as evident in Fig. 1) and the diffraction properties of the system [17].

This correlation/anticorrelation boundary may be shown to persist to the far field $(z_d \gg kw^2/2)$, where the MCF is given by [18]

$$\Gamma'(\vec{f}_1, \vec{f}_2) = (1/\lambda z_d)^2 \iiiint \Gamma(\vec{r}_1, \vec{r}_2)$$
$$\times \exp[-i2\pi(\vec{f}_1 \cdot \vec{r}_1 - \vec{f}_2 \cdot \vec{r}_2)]d\vec{r}_1 d\vec{r}_2, \qquad (7)$$

where $\vec{f}_i = \vec{r}_i'/\lambda z_d$ $(i = 1, 2)$. Numerical integration of Eq. (7) allows us to visualize the far-field intensity distribution, $I'(\vec{f}) \equiv \Gamma'(\vec{f}_1, \vec{f}_1)$. The case $m = 1$ is shown in Figs. 2(a)–2(c) for different states of coherence. The high coherence case produces a dark vortex core with a minimum intensity that is close to zero as expected. In the partial and low coherence cases, the core fills with diffuse light. In contrast, the far-field cross-correlation function, $\chi'(\vec{f}) \equiv \Gamma'(\vec{f}_1, -\vec{f}_1)$, shown in Figs. 2(d)–2(f), maintains attributes of a singularity as the spatial coherence is decreased. In each case, $\chi'(\vec{f})$ exhibits a ring phase dislocation of radius f_r that is characterized by a π phase
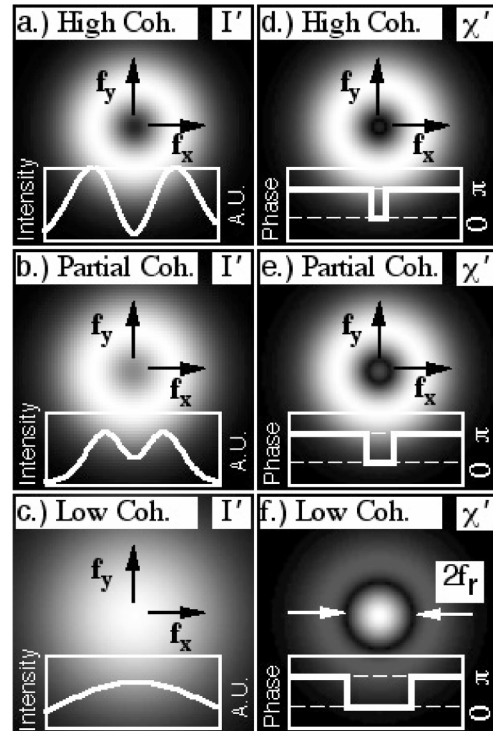

FIG. 2. Numerically computed intensity (a)–(c) and cross-correlation (d)–(f) functions for $m = 1$ in the far-field plane for various coherence lengths. As the coherence decreases, the dark vortex core fills with diffuse light. However, a ring dislocation persists in the cross-correlation function, and its radial size, f_r, increases with decreasing coherence.

step across the circular boundary where $\chi'(\vec{f})$ is zero. Inside (outside) the ring the numerical value of $\mathrm{Re}[\chi'(\vec{f})]$ is positive (negative).

At any distance, z_d, the spatial distribution of $\mathrm{Re}[\chi'(\vec{r}')]$ may be obtained with the aid of a wavefront folding (WFF) interferometer [19]. The expected interferogram is given by

$$F(x', y') = I(-x', y') + I(x', -y') \\ + 2\mathrm{Re}[\langle E(-x', y')E^*(x', -y')\rangle]\cos(\Delta\vec{k}_\perp \cdot \vec{r}'), \tag{8}$$

where $\Delta\vec{k}_\perp$ is the difference between the wave vectors of the two beams emerging from the interferometer. Owing to the symmetry of our system, $E(-x', y') = E(x, y)\exp(i\pi)$ and $E(x, -y) = E(-x, -y)\exp(i\pi)$, hence the cross term in Eq. (8) becomes $2\mathrm{Re}[\chi'(\vec{r}')]\times\cos(\Delta\vec{k}_\perp \cdot \vec{r}')$. The magnitude and phase of $\mathrm{Re}[\chi'(\vec{r}')]$ is found by measuring the fringe visibility and deformation, respectively. At the boundary of a ring dislocation in $\chi'(\vec{r}')$, the fringe visibility is expected to vanish and the π phase shift across the boundary turns bright fringes dark.

We obtained the cross-correlation function of a vortex beam with the apparatus shown in Fig. 3. Broadband light from a halogen bulb was passed through two apertures placed a distance $S = 41.5$ cm apart. The spatial coherence of the source was controlled by varying the size of the aperture, Ap_1. Assuming the beam in the Ap_1 plane is spatially incoherent, the transverse coherence length in the second aperture plane is approximately given by $L_c = 0.64\lambda_{\mathrm{ave}}S/R_s$, where λ_{ave} is the average wavelength, and R_s is the radial size of Ap_1 [17]. The second aperture, Ap_2,
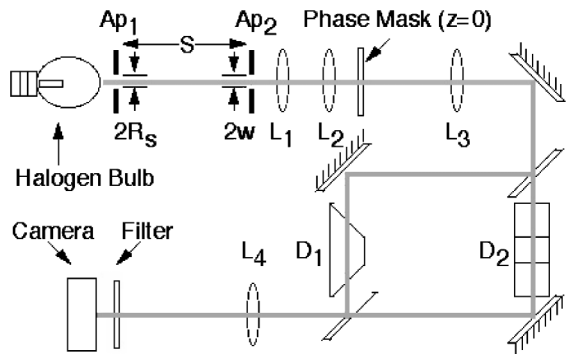

FIG. 3. A schematic diagram of the experiment showing light from a halogen bulb with a mean wavelength of 800 nm and a bandwidth of 50 nm passing through two apertures separated by a distance, $S = 41.5$ cm. The Ap_2 plane was imaged with unity magnification by two 50.2 mm focal length lenses (L_1 and L_2) onto a phase mask designed to produce an $m = 1$ vortex beam. The plane $z = 92$ mm was imaged with a magnification of 3 by two lenses having focal lengths $f = 125$ mm (L_3) and $f = 500$ mm (L_4) onto a CCD camera after passing through a wavefront folding interferometer comprising Dove prisms, D_1 and D_2.

had a radial size $w = 2.5$ mm. Lenses L_1 and L_2 imaged Ap_2 with unity magnification onto a vortex phase mask. Our mask resembled a spiral staircase having 16 steps, each differing in phase from its adjacent neighbor by $\pi/8$. The fused silica mask was designed to produce a vortex of charge $m = 1$ at $\lambda_0 = 890$ nm at an air interface, although we found it also produces an $m = 1$ vortex at wavelengths shorter than 800 nm [20]. At a distance $z_d = 92$ mm from the mask the beam was imaged onto a camera using lenses L_3 and L_4. The WFF interferometer was created by placing Dove prisms, D_1 and D_2, in each arm of a Mach-Zender interferometer. These prisms inverted the beam in one arm across the x axis [$E_1(x', y') = E(-x', y)$] and the other arm across the y axis [$E_2(x', y') = E(x', -y')$]. A Meade Pictor model 416XT astronomical camera recorded the interferograms. A 50 nm bandpass filter with a mean transmitted wavelength of $\lambda_{\mathrm{ave}} = 800$ nm was placed in front of the camera to eliminate temporal coherence effects (e.g., fringe fading).

During the experiment we varied R_s from 0.25 to 1.5 mm in 0.125 mm steps with a precision of ± 0.005 mm. At the largest transverse coherence length, the predicted ring dislocation was barely detectable. As the value of R_s was increased, the ring of zero fringe visibility increased in size. Meanwhile the area of high fringe visibility (i.e., the coherence area) decreased in size. We note that another ring dislocation attributed to the Airy disk is expected to bound the coherence area [21]. From our experimental interferograms, these rings coincided when $R_s = 0.89$ mm (i.e., $L_c = 0.25$ mm).

Two typical experimental images obtained with $R_s = 0.5$ mm (i.e., $L_c = 0.5$ mm) may be seen in Fig. 4(a) for $m = 1$ and Fig. 4(b) for $m = 0$. A ring of zero fringe visibility of radial size R' is seen within the coherence area in Fig. 4(a). Bright fringes inside the ring are shifted to dark fringes outside the ring, indicating a π phase shift occurs across the ring. A corresponding ring is not seen in Fig. 4(b). Although the intensity appears lower inside the ring dislocation in Fig. 4(a), the value of the fringe
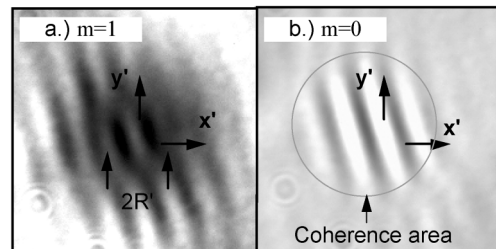

FIG. 4. Experimental interferograms of the cross-correlation function in the plane $z = 540$ mm for an (a) $m = 1$ vortex beam and (b) $m = 0$ nonvortex beam ($L_c/w = 0.20$ in both cases). Shifted (a) and uniform (b) fringes indicate the respective presences and absences of a ring dislocation of radial size, $R' = 0.08$ mm.
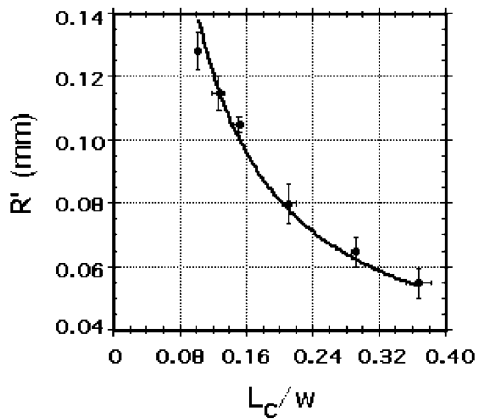
FIG. 5. Experimental (points) and theoretical (line) values of the dislocation radius R' in the measurement plane as a function of the relative coherence length L_c/w at the entrance face of the vortex mask.

visibility was 0.36 ± 0.05 (0.11 ± 0.05) inside (outside). This difference in fringe visibility qualitatively agrees with the results shown in Fig. 2(f).

The average of five measurements made of R' and L_c were calculated and plotted in Fig. 5. The transverse coherence length, L_c, was measured at the plane $z = 0$ (shown in Fig. 3) by removing the mask and then replacing lens L_4 with a 250 mm focal length lens, which imaged the plane $z = 0$ onto the CCD camera. The ring radius R' a distance z_d from the mask may be approximated by [17]

$$R'(z_d) = R(0) + (2\pi)^{1/2}(z_d/kL_c), \qquad (9)$$

where $R(0)$ is the initial size of the ring in the mask plane. Ideally $R(0) = 0$, but due to a slight misalignment of the mask we measured $R(0) = 0.021$ mm. As seen in Fig. 5, we have excellent agreement between the measured (data points) and predicted (solid line) values of R' at difference values of the coherence length.

In conclusion, we find that, although the dark core of an optical vortex diffuses and becomes inconspicuous in incoherent light, the cross-correlation function maintains a ring dislocation that persists regardless of the size of the transverse coherence length. This ring dislocation was characterized by an island of positively correlated light that increases in area with increasing beam spread.

We thank Professor Galina Kitrova for the vortex phase mask used in our experiments. This work was

[1] J. F. Nye and M. V. Berry, Proc. R. Soc. London A **336**, 165 (1974).
[2] For a list of the many works in this area, see G. A. Swartzlander, Jr., Singular Optics/Optical Vortex References, http://www.u.arizona.edu/~grovers/SO/so.html.
[3] V. Yu. Bazhenov, M. V. Vasnetsov, and M. S. Soskin, Zh. Eksp. Teor. Fiz. **52**, 1037 (1990) [Sov. Phys. JETP **52**, 429 (1990)].
[4] N. R. Heckenberg, R. McDuff, C. P. Smith, and A. G. White, Opt. Lett. **17**, 221 (1992).
[5] Z. S. Sacks, D. Rozas, and G. A. Swartzlander, Jr., J. Opt. Soc. Am. B **15**, 2226 (1998).
[6] M. W. Beijersbergen, R. P. C. Coerwinkel, and J. P. Woerdman, Opt. Commun. **112**, 321 (1994).
[7] F. B. Colstoun, G. Khitrova, A. V. Fedorov, T. R. Nelson, C. Lowery, T. M. Brennan, B. G. Hammons, and P. D. Maker, Chaos Solitons Fractals **4**, 1575 (1995).
[8] F. Gori, M. Sanatarsiero, R. Borghi, and S. Vicalvi, J. Mod. Opt. **45**, 539 (1998).
[9] S. A. Ponomarenko, J. Opt. Soc. Am. A **18**, 150 (2001).
[10] Z. Bouchal and J. Perina, J. Mod. Opt. **49**, 1673 (2002).
[11] G. V. Bogatyryova, C. V. Fel'de, P. V. Polyanskii, S. A. Ponomarenko, M. S. Soskin, and E. Wolf, Opt. Lett. **28**, 878 (2003).
[12] G. Gbur and T. D. Visser, Opt. Commun. **222**, 117 (2003).
[13] H. F. Schouten, G. Gbur, T. D. Visser, and E. Wolf, Opt. Lett. **28**, 968 (2003).
[14] G. A. Swartzlander, Jr., Opt. Lett. **26**, 497 (2001).
[15] David Palacios, David Rozas, and Grover A. Swartzlander, Jr., Phys. Rev. Lett. **88**, 103902 (2002).
[16] *Optical Vortices*, edited by M. Vasnetsov and K. Staliunas, Horizons in World Physics Vol. 228 (Nova Science, New York, 1999).
[17] A. S. Marathay, *Elements of Optical Coherence Theory* (Wiley and Sons, New York, 1982).
[18] J. W. Goodman, *Statistical Optics* (John Wiley and Sons, New York, 1985), Sect. 5.4.1.
[19] L. Mertz, *Transformations in Optics* (Wiley, New York, 1965).
[20] David Palacios and Grover Swartzlander, Jr., in *Proceedings of the OSA Annual Meeting & Exhibit, 2002*, OSA Conference Program (Optical Society of America, Washington DC, 2002), p. 121.
[21] B. J. Thompson and E. Wolf, J. Opt. Soc. Am. **47**, 895 (1957).